

Drip Irrigation Water Distribution Patterns: Effects of Emitter Rate, Pulsing, and Antecedent Water

Todd H. Skaggs*

USDA-ARS
U.S. Salinity Lab.
450 W. Big Springs Rd.
Riverside, CA 92507

Thomas J. Trout

USDA-ARS
Water Management Research Unit
Fort Collins, CO 80526

Yuri Rothfuss

USDA-ARS
Water Management Research Unit
Parlier, CA 93648

Drip irrigation is more effective and less expensive if a large amount of soil can be wetted with each emitter without losing water or nutrients below the root zone. The distance that water spreads horizontally from a drip line and the volume of soil wetted are limiting factors that determine the spacing and number of drip lines and emitters, the frequency of irrigation, and thus the cost of irrigation. We used numerical simulations and field trials to investigate the effects of application rate, pulsed water application, and antecedent water content on the spreading of water from drip emitters. Simulation results showed that pulsing and lower application rates produced minor increases in horizontal spreading at the end of water application. The small increases were primarily due to longer irrigation times, however, and not to flow phenomena associated with pulsing or low application rates. Moreover, the small increases mostly disappeared after the infiltrated water had redistributed for a period of 24 h. Field trials confirmed the simulation findings, with no statistically significant difference in wetting being found among five water application treatments involving pulsed applications and varying application rates. The simulations showed that higher antecedent water content increases water spreading from drip irrigation systems, but the increases were greater in the vertical direction than in the horizontal, an undesirable outcome if crop roots are shallow or groundwater contamination is a concern. Overall, soil texture (hydraulic properties) and antecedent water content largely determine the spreading and distribution of a given water application, with pulsing and flow rate having very little impact.

Drip irrigation is an increasingly popular method of irrigation. In the United States, drip irrigation (excluding microspray) is used on about 950,000 ha (National Agricultural Statistics Service, 2009, Table 6) and is the predominant form of irrigation on some high-value fruit and vegetable crops such as grape (*Vitis vinifera* L.), strawberry (*Fragaria* × *ananassa* Duchesne ex Rozier), tomato (*Solanum lycopersicum* L.), melon (*Cucumis melo* L.), and pepper (*Capsicum annuum* L. var. *annuum*). Drip irrigation systems can deliver water efficiently and uniformly to emitters distributed around a field; however, delivery of the water from each emitter throughout the rooting zone depends on soil hydraulic properties.

A constraint of drip irrigation is the number of emitters and laterals required to adequately deliver water to plant roots, as well as any nutrients or pesticides applied with the water. When horizontal water spreading is low, more emitters and laterals are required and system costs are higher. Larger water applications produce greater spreading, but in both the horizontal and vertical directions. Increased vertical spreading may be undesirable because water moving below the active root zone can result in wasted water, loss of nutrients, and groundwater pollution. Thus the goal is to maximize the relative horizontal to vertical water movement for a given water application. Relative horizontal water movement is lowest in well-drained, coarse-textured soils, such as are found where many annual fruit and vegetable crops are grown with drip irrigation.

Mention of products and trade names are for the benefit of the reader and do not imply a guarantee or endorsement of the product by USDA.

Soil Sci. Soc. Am. J. 74:1886–1896
Published online 1 Sept. 2010
doi:10.2136/sssaj2009.0341
Received 9 Sept. 2009.

*Corresponding author (Todd.Skaggs@ars.usda.gov).

© Soil Science Society of America, 5585 Guilford Rd., Madison WI 53711 USA

All rights reserved. No part of this periodical may be reproduced or transmitted in any form or by any means, electronic or mechanical, including photocopying, recording, or any information storage and retrieval system, without permission in writing from the publisher. Permission for printing and for reprinting the material contained herein has been obtained by the publisher.

One specific case where horizontal wetting is critical is drip application of pesticides such as soil fumigants, an increasingly popular method of controlling pathogens, nematodes, and weeds (Ajwa et al., 2002; Trout, 2006). In California, approximately 5000 ha of farmland was drip fumigated in 2005, and at present more than half of the strawberry acreage is drip fumigated (Ajwa et al., 2008). Drip fumigation is potentially safer than other methods of application (e.g., shank injection) because it requires fewer workers in the field during application (Ajwa et al., 2008) and may also result in lower amounts of toxic gases emitted into the atmosphere (Gan et al., 1998; Wang et al., 2001; Papiernik et al., 2004).

When fumigant and other pesticides are applied through a drip irrigation system, they are distributed through the soil by the infiltrating water, with little movement beyond the wetted area (Ajwa and Trout, 2004). Control of pests and pathogens is thus maximized when the entire root zone is wetted by the drip system. The extent of horizontal spreading determines how closely emitters and tubing must be spaced to get complete treatment of a planting bed, and thus how many drip laterals must be used and how much the system costs (Trout et al., 2005).

Factors affecting the spread of water from drip sources include various soil physical properties such as texture and structure (e.g., Warrick, 1974; Bresler, 1978; Cote et al., 2003; Thorburn et al., 2003; Gärdenäs et al., 2005). It has also been suggested that certain management techniques such as pulsed applications, high application rates, and preirrigation of soil beds may increase horizontal spreading of water and chemicals (e.g., Li et al., 2004). For example, some irrigation guidelines indicate that the emitter rate will significantly affect the horizontal/vertical ratio of the wetted soil, with a higher emitter rate increasing the ratio (e.g., Brouwer et al., 1988, Fig. 64). These guidelines were developed based on surface drip irrigation systems in which high application rates cause water to pond and spread across the soil surface (Brandt et al., 1971; Bresler, 1978; Gärdenäs et al., 2005). When water ponds on the soil surface, however, control of the water distribution is jeopardized and surface evaporation loss increases. Surface ponding when applying fumigants is not allowed.

Water distributions emanating from subsurface drip sources under varying management scenarios were investigated in a modeling study by Cote et al. (2003). They performed numerical simulations of drip irrigation, which indicated that decreasing the discharge rate slightly increased the dimensions of the wetted region, contrary to the surface drip guidelines noted previously. It is not clear, however, that the increases in wetting observed by Cote et al. (2003) were large enough to be of practical consequence, particularly because the observations were made at the end of the simulated water applications and before any water redistribution had occurred, which tends to reduce any differences in wetting (e.g., Skaggs et al., 2004). Cote et al. (2003) also investigated pulsed water applications, which have been used in the past to obtain low, quasi-constant water application rates (Zur, 1976; Zur and Savaldi, 1977; Assouline et al., 2006; Wang et al., 2006). Pulsing, according to Cote et al. (2003), is also “commonly perceived” to increase the

lateral extent of wetting. They concluded from their simulations, however, that pulsing has very little impact on water distribution.

As reviewed by Lubana and Narda (2001), a considerable literature exists on modeling water distributions under drip irrigation, including analytical models (e.g., Warrick, 1974; Bresler, 1978; Andreas et al., 1993; Coelho and Or, 1997; Mmolawa and Or, 2000; Cook et al., 2003, 2006) and numerical simulations (e.g., Brandt et al., 1971; Cote et al., 2003; Leib and Jarrett, 2003; Skaggs et al., 2004). A number of the more recent numerical studies (e.g., Assouline, 2002; Cote et al., 2003; Skaggs et al., 2004; Gärdenäs et al., 2005; Lazarovitch et al., 2007; Provenzano, 2007; Dudley et al., 2008; Roberts et al., 2009) have utilized the HYDRUS-2D simulation model (Šimůnek et al., 1999). Skaggs et al. (2004) compared HYDRUS-2D simulations of drip irrigation with measured field data and concluded that the simulations were sufficiently accurate to permit the meaningful study of drip management techniques.

In this work, we used a combination of HYDRUS-2D simulations and field trials to determine the degree to which management practices related to application rate, pulsing, and antecedent water can be used to affect horizontal water spreading from drip irrigation emitters. We considered water distributions emanating from thin-walled drip tubing installed just a few centimeters below the soil surface, a common irrigation system for the production of annual fruit and vegetable crops. The shallow burial protects the tubing and holds it in place, while allowing relatively easy removal at the end of the year. Because such a small amount of soil exists above the line, the water distributions emanating from a shallow placement resemble “surface” drip irrigation rather than “subsurface,” where burial is typically deeper.

MATERIALS AND METHODS

Numerical Simulations

Simulations of water infiltration and redistribution under drip irrigation were performed using HYDRUS-2D (Šimůnek et al., 1999). The simulations followed the same approach used by Skaggs et al. (2004), which we briefly summarize here. The HYDRUS-2D code simulates variably saturated water flow by solving the Richards equation using a finite-element method. The van Genuchten model of the soil hydraulic properties (water retention and hydraulic conductivity functions) was used. The hydraulic parameter values estimated by Skaggs et al. (2004) for their field site, a Hanford sandy loam soil (coarse-loamy, mixed, superactive, nonacid, thermic Typic Xerorthent) were: residual water content $\theta_r = 0.021 \text{ m}^3 \text{ m}^{-3}$, saturated water content $\theta_s = 0.34 \text{ m}^3 \text{ m}^{-3}$, saturated hydraulic conductivity $K_s = 1.6 \text{ cm h}^{-1}$, and van Genuchten shape parameters n , α , and $l = 1.4$, 0.023 cm^{-1} , and -0.92 , respectively; these same parameter values were used in the current simulations so that the results could provide guidance for subsequent field trials that are described below.

We assumed that a drip line with closely spaced emitters operates as a uniform line source, such that infiltration and redistribution are two dimensional, occurring in the vertical plane perpendicular to the drip line. Skaggs et al. (2004) found that this was an acceptable approximation for the conditions of the current study, including a wetted width that was significantly larger than the emitter spacing and soil water

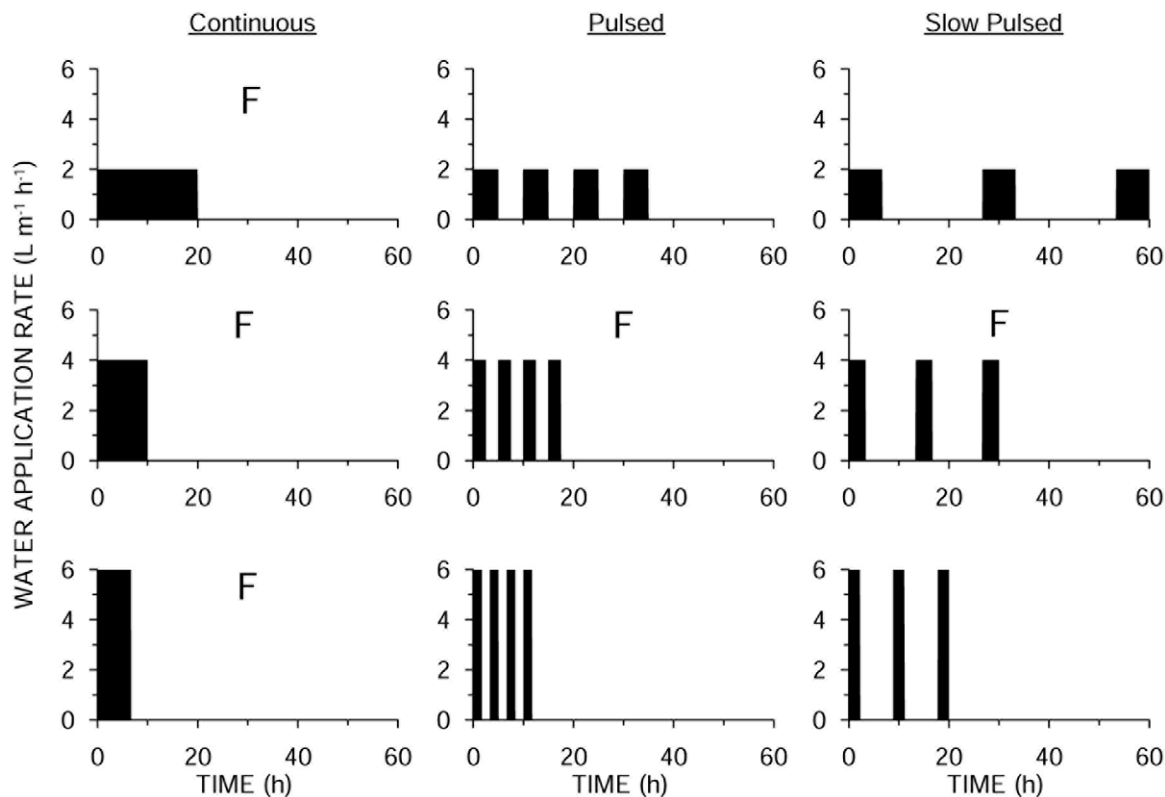


Fig. 1. Water application rates and sequences used in simulations of drip irrigation; F = treatment was also implemented in field trials. All treatments total 40 L m^{-1} applied water.

content measurements that integrated any variability in the direction of the drip line (details of the sampling given below). Only the right side of the vertical profile was simulated (the left side being the mirror image of the right). The boundary of the finite element mesh was rectangular except on the left edge, where a small semicircle curving inward represented the subsurface drip line. The 20-mm-diameter drip line was located 6 cm below the soil surface. The drip line boundary segment was specified as a constant water flux during water application and as a no-flow condition at other times. The left and surface boundaries were also no-flow conditions (due to symmetry considerations and the specification of no evaporation at the surface, respectively). The grid was made large enough (110 by 110 cm) so that the right and bottom boundaries did not affect the simulation results. The simulation method described so far is the same as that used in Skaggs et al. (2004), where additional details were given.

We performed a series of simulations in which three factors were varied: the discharge rate, the initial (antecedent) soil water content, and the application sequence. Three values or treatments were used for each factor, for a total of 27 simulation runs. The discharge rates were 2, 4, and $6 \text{ L m}^{-1} \text{ h}^{-1}$ (equivalent to 2, 4, and 6 mm h^{-1} application rates for drip lines spaced 1 m apart). The spatially uniform initial water contents were 0.06, 0.11, and $0.16 \text{ m}^3 \text{ m}^{-3}$, the latter two water contents corresponding approximately to the water content at 50% plant available water and 33.3 kPa pressure head, respectively. The application sequences were a continuous application, a pulsed application in which water was applied in four equal segments that were interspersed with no-irrigation periods of the same duration (a sequence we refer to as *pulsed*), and a pulsed application in which three equal application periods were interspersed with no-irrigation periods three times longer than the application peri-

ods (*slow pulsed*). The application sequences for the different discharge rates are illustrated in Fig. 1. In all 27 treatments, the total amount of water applied was identical, 40 L m^{-1} of drip tubing (equivalent to 40 mm with 1-m drip line spacing). Using the metrics described below, the simulated soil wetting for each model run was characterized at the conclusion of the final water application and again 24 h later.

Field Experiment

Following the simulation runs, we conducted field trials of five of the irrigation treatments. The experiments were conducted near Parlier, CA, at the USDA-ARS San Joaquin Valley Agricultural Sciences Center. Trials were performed in 2005, between 22 July and 2 September, and between 27 and 30 September. The site was located approximately 500 m from where the field trials of Skaggs et al. (2004) were conducted. In an effort to thoroughly mix the soil profile and eliminate any compacted layers, the Hanford sandy loam soil was deep cultivated to a depth of 0.7 m using 4-cm-wide shanks on 75-cm spacings. Passes were made in two directions. The soil was then chiseled to 0.3 m, disked, and harrowed. Just before the start of the experimental trials, three different 50-m lengths of commercial thin-walled drip tubing (drip tape) were installed 1.5 m apart and approximately 5 cm below the soil surface using commercial drip tubing installation equipment (Universal Shanks, Andros Engineering, Paso Robles, CA). Each length of tubing was subsequently sectioned into 4-m-long segments, which permitted the study of a different water application sequence on different segments. The three types of thin-walled drip tubing used were Toro Aqua-Traxx (Toro Agricultural Irrigation, El Cajon, CA) models EA5060834 (20-cm emitter spacing, $2 \text{ L m}^{-1} \text{ h}^{-1}$ output at line pressure of 38 kPa), EA5060650 (15-cm spacing, $4 \text{ L m}^{-1} \text{ h}^{-1}$ at 63 kPa),



Fig. 2. Photograph of exposed wetting profile with coordinate system etched on the face.

and EA5060867 (20-cm spacing, $6 \text{ L m}^{-1} \text{ h}^{-1}$ at 81 kPa). All tubing had 16-mm outside diameters and 0.15-mm wall thicknesses.

As was the case with the simulations, the total water applied at the end of each irrigation treatment was 40 L m^{-1} of drip tubing. Since each segment of tubing was 4 m, each treatment resulted in an application of 160 L of water. Not all of the treatments considered in the simulations were implemented in the field. For the 2 and $6 \text{ L m}^{-1} \text{ h}^{-1}$ application rates, only the continuous application sequence was investigated (Fig. 1). For the $4 \text{ L m}^{-1} \text{ h}^{-1}$ rate, both continuous and pulsing sequences were tested (Fig. 1). The effect of the antecedent water content was not studied; all trials were performed at the prevailing soil water content, which was about $0.02 \text{ m}^3 \text{ m}^{-3}$ at the soil surface, $0.06 \text{ m}^3 \text{ m}^{-3}$ at the 25-cm depth, and $0.04 \text{ m}^3 \text{ m}^{-3}$ at the 60-cm depth. Four replications of the continuous application treatments were completed, and three replications of the pulse treatments were completed.

Water was supplied to the drip lines from a pressurized supply tank constructed from a 3-m section of 30-cm-diameter polyvinyl chloride pipe. Discharge pressure was regulated with an adjustable pressure regulator to achieve the required flow rate. A graduated sight gauge on the side of the supply tank allowed the discharge flow rate and volume of applied water to be monitored and assure a total 160-L application.

During a trial, opaque corrugated plastic sheeting was laid over the wetted soil surface to reduce surface evaporation (the sheeting is visible near the top of Fig. 2). With a corrugation wavelength of about 5 cm, the sheeting contacted the soil only at a few locations and was presumed to not to affect wetting. No water ponding at the soil surface was observed during any trial.

At the end of each irrigation sequence and approximately 24 h later, the sheeting was temporarily removed and a vertical soil profile perpendicular to the drip tubing was exposed. The profile for the second sampling of each trial (i.e., 24 h after completing irrigation) was exposed by shaving an additional 30 cm of soil from the exposed profile. A grid was lightly etched on the profile and a coordinate system established, with the origin at the soil surface directly above the drip tubing (Fig. 2). The location of the perimeter of the wetted soil was observed on the grid based on the color difference between wet and dry soil and was sketched on graph paper marked with the same coordinate system (the sketches

were later scanned and the perimeter digitized). Soil water content measurements were then made on a grid with 7.5-cm spacing. Measurements were made with a MiniTrase time domain reflectometry (TDR) unit (Soilmoisture Equipment Corp., Santa Barbara, CA), with 30-cm-long probes that were inserted horizontally into the profile face. Because the probe length was longer than the emitter spacing, it was assumed that the probe integrated any water content variability that existed in the direction of the drip tubing and produced a representative measurement of the soil water content. Gravimetric water content was measured on soil samples obtained by pressing a 30-cm-long, 2-cm-diameter, slotted steel soil sampling tube (Oakfield Apparatus Co., Oakfield, WI) horizontally into the profile at selected coordinate positions, using the procedure described in Skaggs et al. (2004). The gravimetric measurements were used to verify the TDR probe measurements.

The soil bulk density was determined at several locations in the soil profile with a Soilmoisture Model 0200 soil sampler (5.7-cm-diameter by 6-cm-long double ring manually inserted into the profile wall). The measured bulk density ranged from 1.45 to 1.52 g cm^{-3} , with an average value of 1.48 g cm^{-3} .

Characterization of Water Distributions

Water distributions for simulated and field-measured profiles were characterized in terms of the horizontal (H) and vertical (V) extents of the wetted area, as well as the ratio H/V . We defined H to be the one-sided profile width, measured horizontally from the vertical line passing through the drip tube to the furthest point on the wetted perimeter, while V was the depth of wetting below the soil surface. The distances H and V for the simulated profiles were determined using an algorithm that identified the portion of the soil in which there had been an increase in water content and determined the maximum distance that that region extended from the x and z axes. For the field profiles, H and V were determined by visual inspection of the wetted perimeter sketches made in the field. Some subjective judgment was required in this procedure; if a profile was nonsymmetric about the vertical axis and H differed on the two sides of the profile, an average value was used.

Additionally, the water distributions were characterized in terms of their moments (Lazarovitch et al., 2007):

$$M_{ij} = \iint x^i z^j \Delta\theta(x, z) dx dz \quad [1]$$

where $\Delta\theta(x, z) = \theta(x, z) - \theta_0(x, z)$, θ is the water content, θ_0 is the initial (antecedent) water content, and x and z are the horizontal and vertical space coordinates, respectively. The zeroth spatial moment M_{00} is equal to the volume of applied water per unit length of drip tubing. The center of mass is located at the coordinate (x_c, z_c) , where $x_c = M_{10}/M_{00}$ and $z_c = M_{01}/M_{00}$. A measure of the spread of the water around its center in the x and z directions is given by $\sigma_x^2 = M_{20}/M_{00} - x_c^2$ and $\sigma_z^2 = M_{02}/M_{00} - z_c^2$, respectively. We also calculated the ratio σ_x/σ_z . Moments were computed using standard quadrature techniques following the interpolation of data onto a uniform computational grid, using triangulation techniques for the simulated data and kriging with a linear variogram for the field data. The digitized wetting perimeters were used in kriging and integrating the field water content data, defining a line outside of which $\Delta\theta = 0$. The initial water content distribution

was assumed to vary only in the z direction, $\theta_0(x,z) = \theta_0(z)$, and a single $\theta_0(z)$, determined by averaging soil water content measurements made outside of the wetted zone, was used in calculations for all trials.

RESULTS AND DISCUSSION

Simulation Results

Results for the simulated water distributions are presented in Fig. 3 and 4. We were interested in determining whether the management factors examined in the simulations affected the geometry of the wetted region and the distribution of water. In particular, we were interested to know whether the relative horizontal to vertical spreading of water could be affected.

Figures 3a to 3d show the horizontal distribution metrics H and σ_x plotted vs. the discharge rate. Figures 3a and 3c are the water distributions simulated at the end of water application, whereas Fig. 3b and 3d are the distributions obtained 24 h later. Figures 3a and 3c indicate that, at the end of water application, both the application sequence and the application rate affected the horizontal spreading of the water. As was the case in the simulations of Cote et al. (2003), decreasing the application rate (and thus increasing the application time) increased horizontal spreading at the end of the irrigation. The effect of the application sequence was that slow pulsing produced the greatest spreading, pulsing produced an intermediate level of spreading, and continuous application produced the least spreading at the end of the irrigation. Figures 3b and 3d show, however, that after the applied water redistributed in the soil for 24 h, the data essentially collapsed onto three curves such that horizontal spreading depended almost exclusively on the antecedent water content, with the application rate and sequence having almost no impact. Thus any initial changes in soil wetting brought about by varying either the application sequence or the application rate were eliminated once the water redistributed in the soil. The observed increase in spreading with higher antecedent water was expected because less pore space was available to hold the applied water.

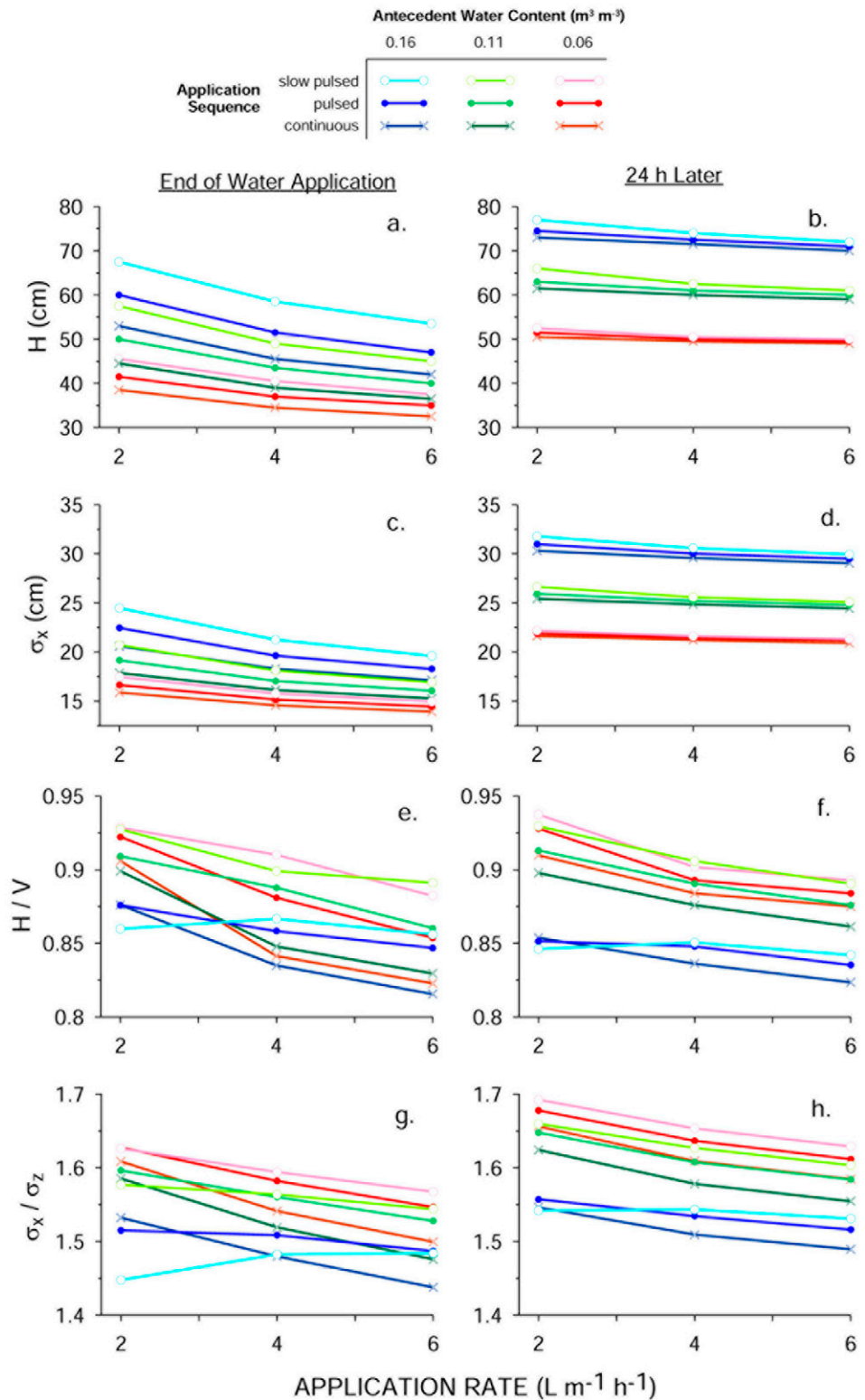


Fig. 3. Values of the parameters (H and V , horizontal and vertical extents, respectively, of the wetted perimeter; σ_x and σ_z , square root of the second central moment in the x and z directions, respectively) characterizing simulated soil water distributions for differing water application rates, application sequences, and antecedent water contents.

Additional insight into the effect of the application rate and sequence on H and σ_x can be gained by plotting the data in Fig. 3 vs. the irrigation time rather than discharge rate. *Irrigation time* is defined to be the time elapsed between the start of irrigation and the completion of the 40 L m^{-1} water application (see Fig. 1).

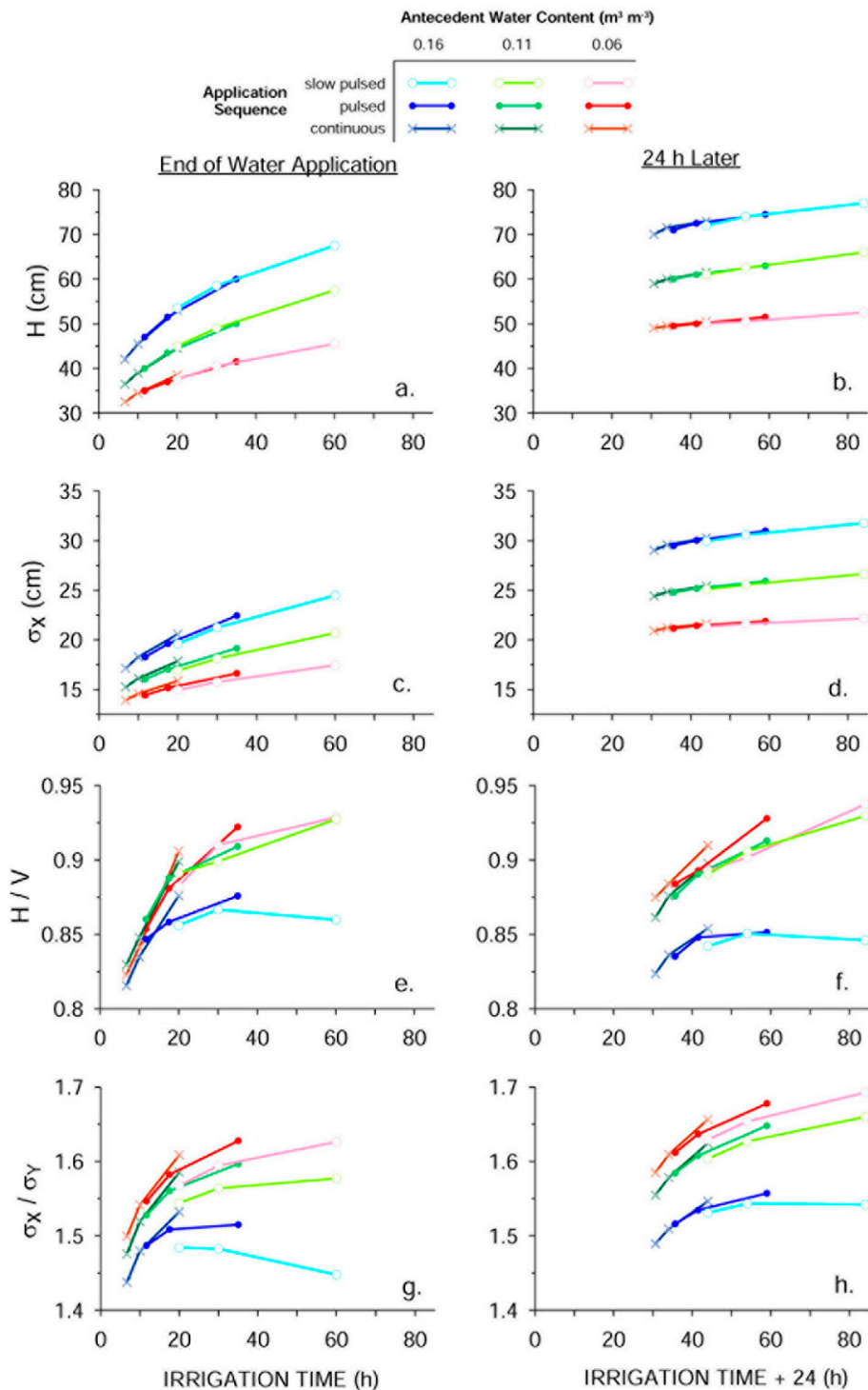


Fig. 4. Values of the parameters (H and V , horizontal and vertical extents, respectively, of the wetted perimeter; σ_x and σ_z , square root of the second central moment in the x and z directions, respectively) characterizing simulated soil water distributions plotted vs. irrigation time. Irrigation time is the elapsed time between the start and end of water application.

Thus for a continuous application, the irrigation time is simply the duration of the water application. For a pulsed application, the irrigation time is the time elapsed between the start of irrigation and the completion of the final water application, including the interspersed periods when water is not being applied. In Fig. 4a and 4c, the data now fall onto one of three curves depending on the antecedent water content. This indicates that H and σ_x at the end of irrigation depended on the application sequence only because of dif-

ferences in the time required to apply the water (i.e., the average application rate). In other words, for a given antecedent water content, any sequence and rate combination requiring, say, 20 h to apply $40 L m^{-1}$ of water would produce, at the end of irrigation, the same horizontal spreading as any other combination also requiring 20 h. This is demonstrated, for example, in Fig. 4a and 4c, where on each curve there are three nearly overlapping data points in the vicinity of 20 h. These data points are for continuous, pulsed, and slow pulsed sequences utilizing differing discharge rates such that the required irrigation times were 20 h, 17.5 h, and 20 h, respectively (see Fig. 1). For these three very different water applications, the horizontal spreading at the end of irrigation was essentially identical because the irrigation times were about the same.

Figures 4b and 4d reaffirm that after 24 h of redistribution, horizontal water spreading for a given antecedent water content was essentially the same for all application rates and sequences. Moreover, those plots show that the small amount of variation in wetting that did exist after 24 h was related to irrigation time, with shorter irrigation times corresponding to less spreading.

The results for relative horizontal spreading, as quantified by H/V and σ_x/σ_z , are shown in Fig. 3e to 3h and 4e to 4h. Excluding a couple of exceptions that will be noted subsequently, the general trends indicated in Fig. 3e to 3h may be summarized as: (i) decreasing the application rate increased the relative horizontal spreading; (ii) decreasing the antecedent water content increased the relative horizontal spreading; (iii) the slow pulsed application sequence produced the largest relative horizontal spreading, followed by the pulsed and continuous sequences, respectively; and (iv) the relative horizontal spreading was slightly greater after 24 h of redistribution compared with the initial water distribution. Exceptions to these trends occurred for the treatments combining the highest antecedent water content ($0.16 m^3 m^{-3}$) with the lower flow rates (4 and especially $2 L m^{-1} h^{-1}$); however, these deviations may be artifacts due to the simulation design and analysis. The uniform initial water content profiles were close to but not completely at equilibrium, and some drainage of antecedent water did occur.

Although the drainage rates were low, some of the pulsed simulations lasted as long as 84 h (Fig. 1), and at the higher initial water contents the downward flow may have been sufficient to affect the water distribution or its delineation, increasing slightly the apparent vertical spreading of the water plume. A small change in V of only a centimeter or two is all that would be required to bring the data points in line with the others.

Figured 4e to 4h demonstrate that the observed variations in H/V and σ_x/σ_z are also related to the irrigation time, with shorter irrigation times corresponding to less relative horizontal spreading. The data in these plots exhibit more scatter than those in the top half of the figure, but the general trends are nevertheless clear. The probable reason for less relative horizontal spreading with shorter irrigation times is that the higher average application rates initially produced higher soil water contents near the drip tube, resulting in greater downward water flow due to gravitational forces.

All of the observed variations indicated in Fig. 3 and 4 for H/V and σ_x/σ_z are relatively minor and not likely to be useful to irrigators trying to affect relative horizontal spreading. The maximum variation among all treatments is 13%, with most variations <10%. As an illustration, Fig. 5 shows the perimeter for two wetted regions with the same V but with H/V ratios that correspond approximately to the simulated range (0.85–0.95). As a practical matter, the difference between those two profiles is probably too small to affect tubing spacing or pollution potential because the difference is probably less than the variation in wetting one would expect to find in a field due to natural soil variability (see, e.g., the field results below). For the simulated soil, it does not seem possible to substantially affect *relative* horizontal spreading through the management of application rate, pulsing, and antecedent water content.

Field Results

Time Domain Reflectometry Calibration

Figure 6a shows the relationship between the apparent dielectric constant (K_a) and volumetric water content (θ). The data points in the figure are the subset of the moisture content data in which water content was measured with both TDR and gravimetric methods. Because no apparent trend in the bulk density data existed, the average value of 1.48 g cm^{-3} was used to convert the gravimetric water content data to volumetric water content. Also shown in Fig. 6a are three curves relating K_a and θ : the default MiniTrase TDR calibration curve, the Topp equation (Topp et al., 1980), and a fitted cubic polynomial. Only marginal differences existed with regard to the agreement of the three curves with the data. We chose to use the default MiniTrase curve to relate K_a to θ .

Figure 6b shows the result of converting K_a to θ with the MiniTrase curve, again using the subset of data for which gravimetric measurements were available. Figure 6b shows that the TDR water contents tended to be higher than the gravi-

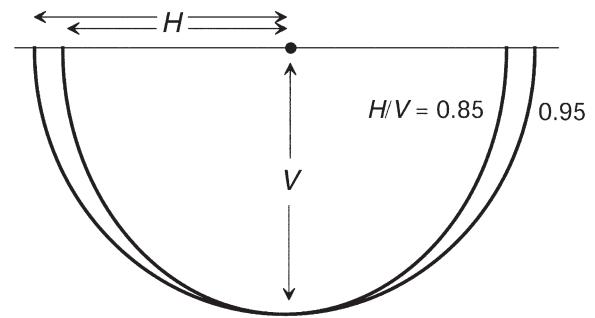


Fig. 5. Schematic illustration of two wetting perimeters with the same vertical extent, V , but differing horizontal extents, H .

metric measurements, especially at very low soil water contents. A least squares linear regression comparison of the TDR and gravimetric data produced a slope that was not significantly different than one, but the intercept was significantly larger than zero (Fig. 6b, $R^2 = 0.94$). When gravimetric water content data <6% were excluded, the slope was not significantly different than 1 and the intercept was not significantly different than zero (Fig. 6b, $R^2 = 0.92$).

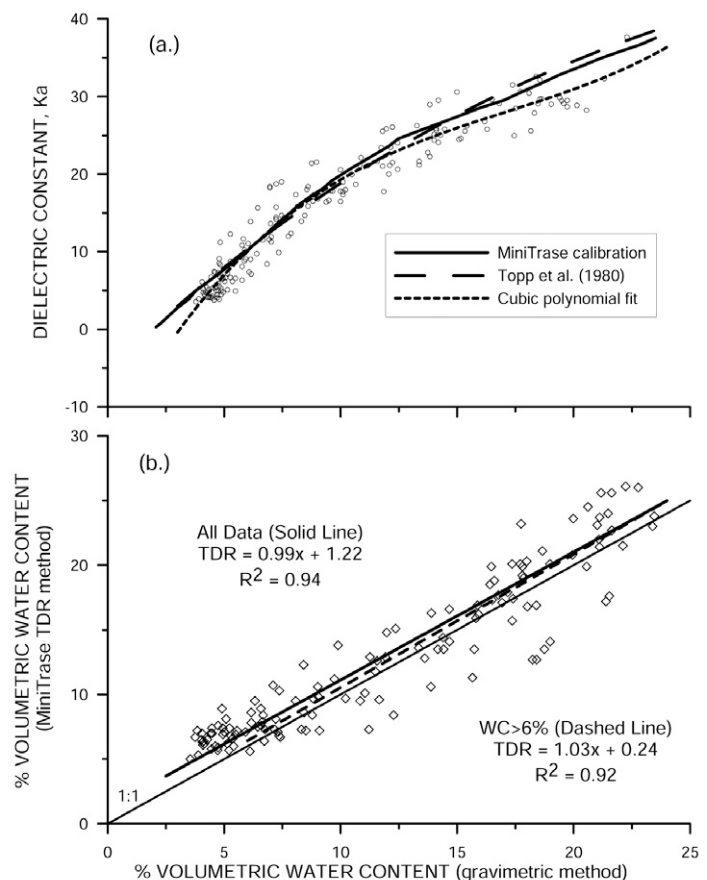


Fig. 6. (a) Relationship between the apparent dielectric constant (K_a) and gravimetrically determined volumetric water content (θ). The three curves shown along with the measured data are: the default MiniTrase time domain reflectometry (TDR) calibration curve; the Topp equation $\theta(\%) = (-530 + 292K_a - 5.5K_a^2 + 0.043K_a^3)10^{-2}$ (Topp et al., 1980); and the fitted cubic polynomial equation $\theta(\%) = (-1488 + 559K_a - 27K_a^2 + 0.52K_a^3)10^{-2}$; and (b) a comparison of volumetric water contents measured with the MiniTrase TDR and gravimetric methods.

Water Distributions

Although the procedures used in the current field experiment were very similar to those used previously by Skaggs et al. (2004), it was apparent during the experiment that some differences existed in the observed wetting compared with the earlier study. Whereas the wetting perimeters observed by Skaggs et al. (2004) resembled approximately a semicircle as predicted by theory for homogeneous soils and line sources close to the surface, the current experiment produced in many instances wetting perimeters that appeared “pinched in” near the surface and were more elliptical in shape than semicircular. A greater degree of asymmetry was also observed in the wetting profiles of the current experiment. Several factors probably contributed to these differences. First, during the current experiment, the average daytime high temperature was 36°C, with low relative humidity and only 1 cm of cumulative precipitation. Due to these atmospheric conditions and pre-experiment tillage, the top few centimeters of the soil were extremely dry and appeared to absorb water relatively slowly, probably due to its very low hydraulic conductivity and possibly due to a degree of hydrophobicity. The result was a wetting perimeter that appeared pinched in near the surface, especially at the time of the second sampling (24 h after the end of water application). An example is shown in the lower left plot of Fig. 7. Second, the pre-experiment soil cultivation appeared to be only partially successful in homogenizing the soil. In several trials, a lower conductivity soil layer at a depth of about 30 to 40 cm appeared to slow downward

penetration of the infiltrating water. Lastly, the initial volumetric water content varied with depth: between 2 and 3% in the top 10 cm (approximately), about 4% between 10 and 20 cm, about 6% between 20 and 35 cm, and 3 or 4% below 35 cm. The higher conductivity of the moister layer between 20 and 35 cm probably impacted the shape of the wetting perimeter (demonstrated below).

In total, 18 field trials were run using five treatments: four replications each of the 2, 4, and 6 L m⁻¹ h⁻¹ continuous treatments and three replications of the pulsed and slow pulsed treatments, with all pulse treatments being conducted at an application rate of 4 L m⁻¹ h⁻¹. For each trial, the water distribution was measured at the end of water application and again 24 h later, for a total of 36 measured water distributions. Parameter values characterizing the measured water distributions for the five experimental treatments are given in Table 1. The parameters reported are M_{00} , x_c , z_c , σ_{x^2} , σ_x/σ_z , H , and H/V .

The volumes of applied water estimated by the calculated zeroth spatial moments (M_{00}) of the 36 measured distributions ranged from 25 to 43 L m⁻¹, with an average value of 33 L m⁻¹ and a standard deviation of 4.4 L m⁻¹ (Table 1). The water volumes calculated for the 18 distributions measured at the end of water application were lower than those calculated for distributions obtained after 24 h of redistribution, 31 vs. 34 L m⁻¹ (significant at the 0.05 probability level). The reason the calculated water volumes were, on average, lower than the actual applied value of 40 L m⁻¹ is unknown, but several factors may have con-

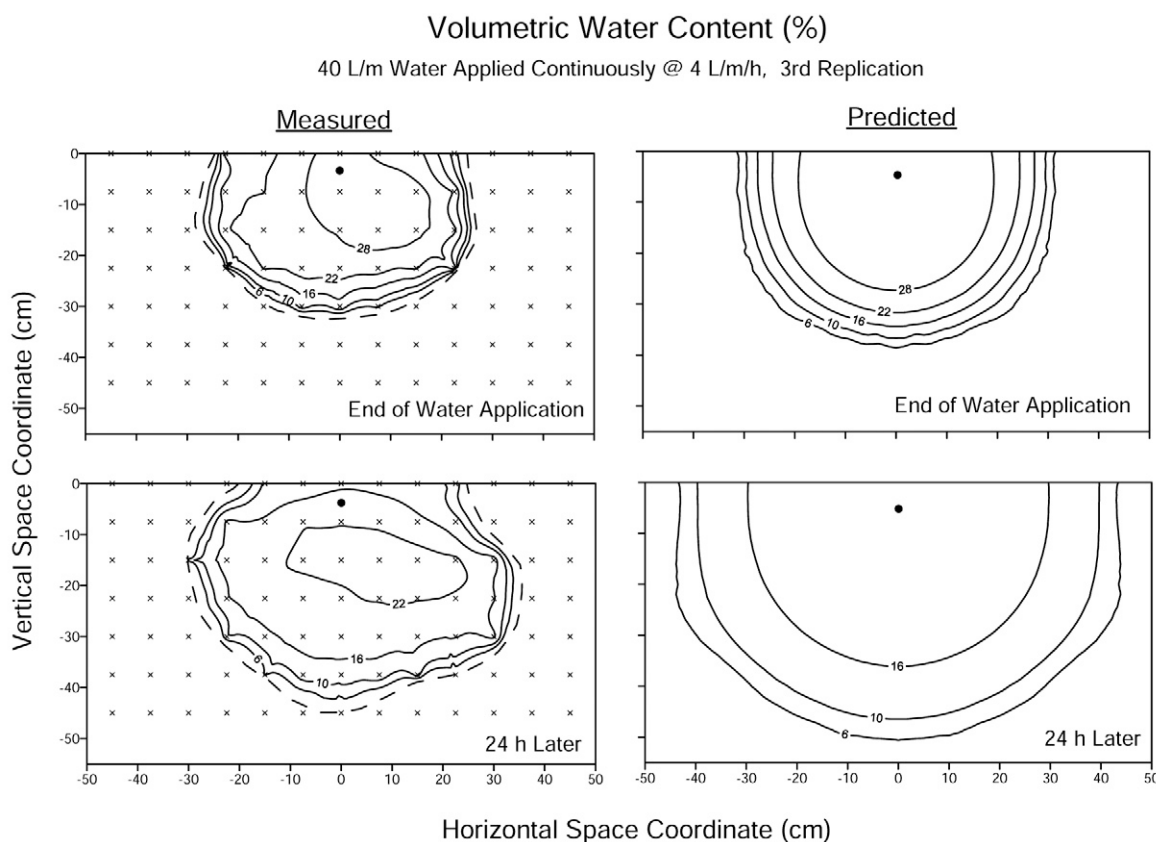


Fig. 7. Sample pair of measured and predicted water distributions for a continuous application at a rate of 4 L m⁻¹ h⁻¹. The filled circles show the position of the drip line. In the measured profile plots, the dashed line indicates the observed wetting perimeter and the × symbols show the locations of the water content measurements.

Table 1. Water distribution parameter† obtained from field trials with 40 L m⁻¹ water application.

Water application			M_{00}	x_c	z_c	σ_x	σ_x/σ_z	H	H/V
Sequence	Rate	Trials							
	L m ⁻¹ h ⁻¹	no.	L m ⁻¹	cm				cm	
First sampling (end of water application)									
Continuous	2	4	31 ± 5‡	0.3 ± 2	15 ± 3	14 ± 2	1.7 ± 0.4	33 ± 6	0.94 ± 0.2
Continuous	4	4	32 ± 8	0.3 ± 1	15 ± 4	13 ± 1	1.6 ± 0.4	28 ± 3	0.81 ± 0.2
Continuous	6	4	30 ± 6	0.7 ± 2	13 ± 1	13 ± 1	1.6 ± 0.2	29 ± 3	0.85 ± 0.2
Slow pulsed	4	3	31 ± 4	-0.3 ± 1	14 ± 3	14 ± 1	1.6 ± 0.3	30 ± 4	0.85 ± 0.2
Pulsed	4	3	33 ± 2	0.7 ± 1	16 ± 7	13 ± 1	1.4 ± 0.7	30 ± 4	0.76 ± 0.4
Second sampling (24 h later)									
Continuous	2	4	34 ± 11	-0.5 ± 1	18 ± 2	15 ± 2	1.5 ± 0.2	35 ± 3	0.81 ± 0.1
Continuous	4	4	35 ± 12	0.9 ± 2	19 ± 4	16 ± 2	1.5 ± 0.1	35 ± 5	0.77 ± 0.1
Continuous	6	4	34 ± 6	1.6 ± 4	18 ± 3	15 ± 2	1.5 ± 0.3	36 ± 6	0.80 ± 0.1
Slow pulsed	4	3	34 ± 6	-0.4 ± 4	19 ± 8	16 ± 1	1.5 ± 0.3	37 ± 5	0.81 ± 0.1
Pulsed	4	3	34 ± 9	0.6 ± 2	20 ± 5	15 ± 2	1.3 ± 0.2	34 ± 2	0.70 ± 0.1

† M_{00} , zeroth spatial moment; x_c and z_c , horizontal and vertical coordinate locations, respectively, of center of mass; σ_x and σ_z , square root of the second central moment in the x and z directions, respectively; H and V , horizontal and vertical extents, respectively, of the wetted perimeter.

‡ 95% confidence intervals computed according to Student's t distribution.

tributed to the discrepancy. As noted above, the TDR measurements tended to overestimate the soil water content, especially at very low water content (Fig. 6). Overestimating the initial water content, θ_0 , would lead to an underestimation of the applied water, M_{00} (see Eq. [1]). For example, if the wetted soil in the exposed profile had an area of 0.15 m², overestimating θ_0 by 0.02 m³ m⁻³ would result in an underestimation of M_{00} by 3 L m⁻¹ (assuming the wetted soil water content, θ , was measured accurately). Another possible factor was that the corrugated plastic did not completely eliminate evaporative water losses. Calculations done with HYDRUS-2D indicated that evaporation could have accounted for a 1 to 3 L m⁻¹ loss of water depending on the assumed effective evaporation rate. On the other hand, both the TDR and evaporation explanations of the error are inconsistent with the observation that the error was larger in the first sampling: both mechanisms should have led to a larger error in the second sampling due a larger wetted area in the case of TDR and a longer elapsed time in the case of evaporation. A third possible contributing factor for the error is that the 7.5- by 7.5-cm sampling grid was not sufficient to permit an accurate interpolation and integration of the water distribution. In this case, the error might be greater in the first sampling because steeper water content gradients existed. In sum, while we speculate that a number of factors possibly contributed to the mass balance error, the explanations are not completely satisfactory and the actual cause(s) are unknown.

We used ANOVA to assess whether, in either sampling, any of the five experimental treatments produced a significantly different value for any of the parameters shown in Table 1. A one-way ANOVA found that, at the 0.1 level, none of the observed parameters were significantly different in any of the five experimental treatments. Thus, consistent with the simulation results, neither pulsing nor the application rate had a significant effect on the observed water distribution, particularly the relative horizontal water spreading.

Comparison of Field Data with Model Predictions

So that the field results could be compared quantitatively with the model predictions, we reran the model simulations using the field-measured initial water content distribution instead of the uniform distribution assumed in the simulations above. Figure 7 shows contour plots for a typical pair of measured and predicted water distributions. Figure 8 compares the predicted water distribution parameter values with the values determined from the field measurements. Figures 8e to 8j show that predictions for relative horizontal spreading (H/V and σ_x/σ_z) and the depth of the center of mass (z_c) were generally consistent with the field data; however, Fig. 8a to 8d show that horizontal water spreading in the field was less than predicted by the model, particularly in the distributions measured 24 h after the end of water application. At the end of water application, the predictions of H and σ_x were above the field mean value for all five irrigation treatments, although in three of the treatments the predicted values fell within the estimated 95% confidence bounds (Fig. 8a and 8c). On the other hand, predictions of H and σ_x for the later distributions were all well above the estimated confidence intervals for the field values (Fig. 8b and 8d).

The reason for the disagreement between the data and model predictions is not known. The simulations were made assuming a homogeneous soil profile with hydraulic properties taken from Skaggs et al. (2004). It is likely that computations made with site-specific hydraulic properties, perhaps accounting for the previously noted less conductive layers at the surface and 30- to 40-cm depths, would produce simulated wetting in closer agreement to that observed in the field. In any event, it is interesting to note that the nonuniform initial water content profile, which had a slightly wetter layer at 20 to 35 cm and which perhaps arose in the field due to the less conductive layer at 30 to 40 cm, had some effect on the shape of the simulated wetting perimeters, making them less semicircular than profiles typically obtained under uniform initial conditions. For example, the 6% contour in the lower right plot of Fig. 7 shows a very slight outward bulging between 15 and 25 cm. The effect is minor, but it reinforces the previously noted importance of antecedent water on wetting.

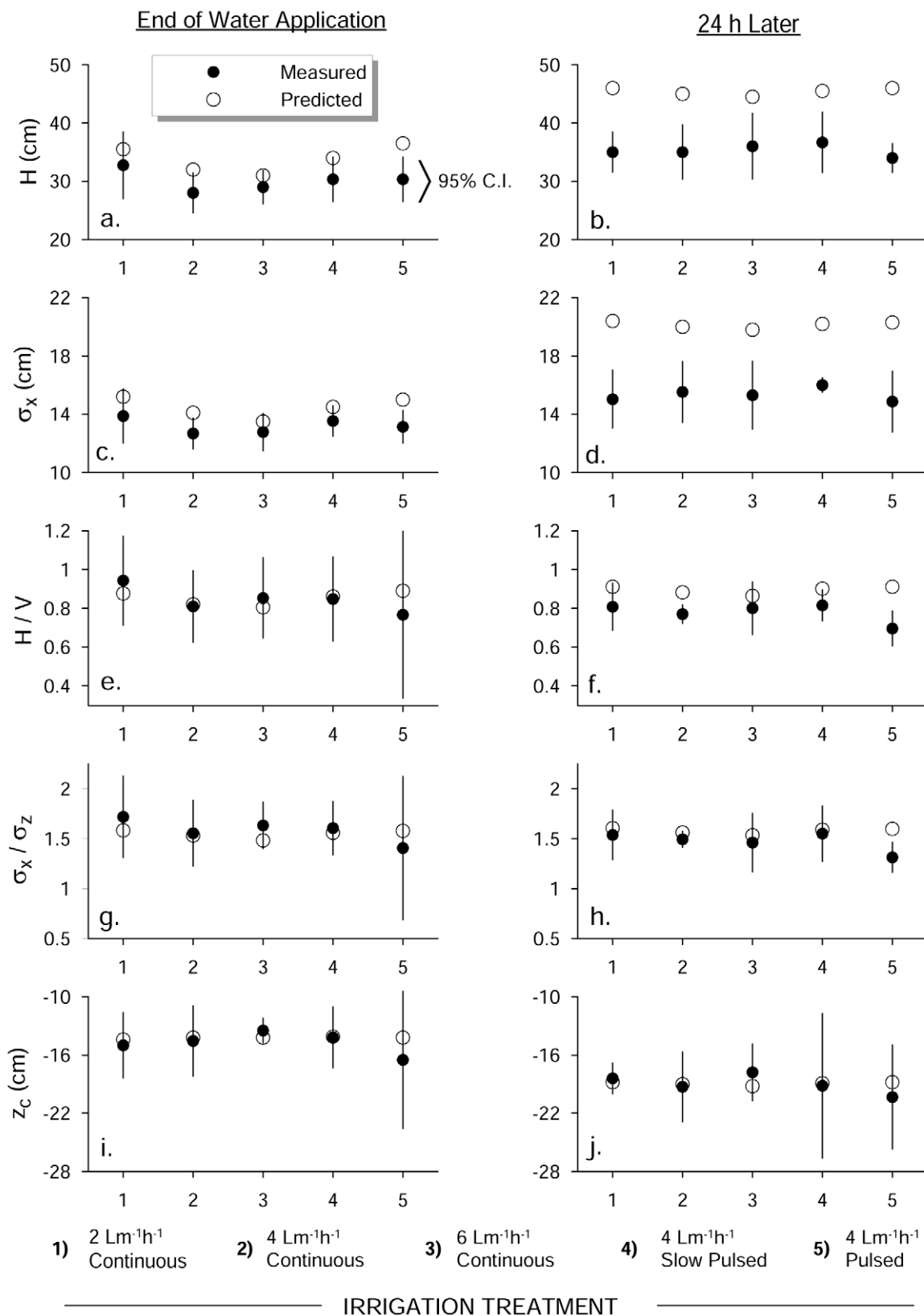


Fig. 8. Comparison of measured and predicted water distribution parameters (H and V , horizontal and vertical extents, respectively, of the wetted perimeter; σ_x and σ_z , square root of the second central moment in the x and z directions, respectively; z_c , depth of center or mass) for differing irrigation rates and sequences.

SUMMARY AND CONCLUSIONS

The distance that water spreads horizontally from a drip line is important because it determines the required emitter spacing, the number of drip lines, and the cost of the system. In this work,

model simulations were used to test the effects of the water application rate, pulsing, and antecedent soil water content on soil wetting from drip systems. Simulations for a Hanford sandy loam soil showed that low antecedent soil water content and low applica-

tion rates, whether achieved by low-discharge emitters or pulsing, slightly increased the relative horizontal to vertical water spreading. The increases were attributable to longer irrigation times and not due to flow phenomena associated with pulsing; however, the effects of pulsing, application rate, and antecedent water on the horizontal/vertical ratio of the wetted soil volume were generally <10% and not large enough to be of practical significance. Increasing the antecedent water content increases water spreading in *both* directions, which is undesirable where root zones are shallow, water is scarce, or groundwater contamination is a concern.

Five of the irrigation treatments investigated in the simulations were tested in field trials. The results confirmed the conclusions of the simulations: none of the treatments involving differing emitter discharge rates and pulsing protocols produced soil wetting that was significantly different from any of the others.

It was not unexpected that drip management parameters other than antecedent soil water content would have only minimal impacts on soil water distributions. Soil hydraulic properties and water content are the primary factors determining the soil capillary forces that drive horizontal water movement. It is not possible, for example, to use higher application rates to “push” water out through soils from drip lines. In fact, as indicated by the simulations here and elsewhere (e.g., Cote et al., 2003), high discharge rates from a subsurface source tend to increase vertical spreading more than horizontal. In practice, the soil wetting that will be realized from drip application of a given volume of water will be determined by the texture (hydraulic properties) of the soil and the antecedent soil water content and will be not be significantly impacted by the discharge rate or pulsing.

REFERENCES

Ajwa, H.A., and T. Trout. 2004. Drip application of alternative fumigants to methyl bromide for strawberry production. *HortScience* 39:1707–1715.

Ajwa, H., T. Trout, and M.P. Bolda. 2008. UC pest management guidelines: Strawberry drip fumigation. *Agric. and Nat. Resour. Publ.* 3468. Available at www.ipm.ucdavis.edu/PMG/r734900211.html (verified 7 Aug. 2010). *Integrated Pest Manage. Progr.*, Univ. of Calif., Davis.

Ajwa, H.A., T. Trout, J. Mueller, S. Wilhelm, S.D. Nelson, R. Soppe, and D. Shatley. 2002. Application of alternative fumigants through drip irrigation systems. *Phytopathology* 92:1349–1355.

Andreas, N.A., D.E. Rolston, T.N. Kadir, and V.H. Scott. 1993. Soil-water distribution under trickle source. *J. Irrig. Drain. Eng.* 119:484–500.

Assouline, S. 2002. The effects of microdrip and conventional drip irrigation on water distribution and uptake. *Soil Sci. Soc. Am. J.* 66:1630–1636.

Assouline, S., M. Möller, S. Cohen, M. Ben-Hur, A. Grava, K. Narkis, and A. Silber. 2006. Soil-plant system response to pulsed drip irrigation and salinity: Bell pepper case study. *Soil Sci. Soc. Am. J.* 70:1556–1568.

Brandt, A., E. Bresler, N. Diner, I. Ben-Asher, J. Heller, and D. Goldberg. 1971. Infiltration from a trickle source: I. Mathematical models. *Soil Sci. Soc. Am. Proc.* 35:675–682.

Bresler, E. 1978. Analysis of trickle irrigation with application to design problems. *Irrig. Sci.* 1:3–17.

Brouwer, C., C. Prins, M. Kay, and M. Heibloem. 1988. *Irrigation water management: Irrigation methods. Training manual no. 5. Provisional ed.* FAO, Rome.

Coelho, F.E., and D. Or. 1997. Applicability of analytical solutions for flow from point sources to drip irrigation management. *Soil Sci. Soc. Am. J.* 61:1331–1341.

Cook, F.J., P. Fitch, P.J. Thorburn, P.B. Charlesworth, and K.L. Bristow. 2006. Modelling trickle irrigation: Comparison of analytical and numerical models for estimation of wetting front position with time. *Environ. Model. Softw.* 21:1353–1359.

Cook, F.J., P.J. Thorburn, P. Fitch, and K.L. Bristow. 2003. *WetUp: A software tool to*

display approximate wetting patterns from drippers. *Irrig. Sci.* 22:129–134.

Cote, C.M., K.L. Bristow, P.B. Charlesworth, F.J. Cook, and P.J. Thorburn. 2003. Analysis of soil wetting and solute transport in subsurface trickle irrigation. *Irrig. Sci.* 22:143–156.

Dudley, L.M., A. Ben-Gal, and N. Lazarovitch. 2008. Drainage water reuse: Biological, physical, and technological considerations for system management. *J. Environ. Qual.* 37:S-25–S-35.

Gan, J., S.R. Yates, D. Wang, and F.F. Ernst. 1998. Effect of application methods on 1,3-dichloropropene volatilization from soil under controlled conditions. *J. Environ. Qual.* 27:432–438.

Gärdenäs, A.I., J.W. Hopmans, B.R. Hanson, and J. Šimůnek. 2005. Two-dimensional modeling of nitrate leaching for various fertigation scenarios under micro-irrigation. *Agric. Water Manage.* 74:219–242.

Lazarovitch, N., A.W. Warrick, A. Furman, and J. Šimůnek. 2007. Subsurface water distributions from drip irrigation described by moment analysis. *Vadose Zone J.* 6:116–123.

Leib, B.G., and A.R. Jarrett. 2003. Comparing soil pesticide movement for a finite-element model and field measurements under drip chemigation. *Comput. Electron. Agric.* 38:55–69.

Li, J., J. Zhang, and M. Rao. 2004. Wetting patterns and nitrogen distributions as affected by fertigation strategies from a surface point source. *Agric. Water Manage.* 67:89–104.

Lubana, P.P.S., and N.K. Narda. 2001. Modelling soil water dynamics under trickle emitters: A review. *J. Agric. Eng. Res.* 78:217–232.

Mmolawa, K., and D. Or. 2000. Water and solute dynamics under a drip-irrigated crop: Experiments and analytical model. *Trans. ASAE* 43:1597–1608.

National Agricultural Statistics Service. 2009. *Farm and ranch irrigation survey (2008)*. Available at www.agcensus.usda.gov/Publications/2007/Online_Highlights/Farm_and_Ranch_Irrigation_Survey/fris08.pdf (verified 7 Aug. 2010). NASS, Washington, DC.

Papiernik, S.K., R.S. Dungan, W. Zheng, M. Guo, S.M. Lesch, and S.R. Yates. 2004. Effect of application variables on emissions and distribution of fumigants applied via subsurface drip irrigation. *Environ. Sci. Technol.* 38:5489–5496.

Provenzano, G. 2007. Using HYDRUS-2D simulation model to evaluate wetted soil volume in subsurface drip irrigation systems. *J. Irrig. Drain. Eng.* 133:342–349.

Roberts, T., N. Lazarovitch, A.W. Warrick, and T.L. Thompson. 2009. Modeling salt accumulation with subsurface drip irrigation using HYDRUS-2D. *Soil Sci. Soc. Am. J.* 73:233–240.

Šimůnek, J., M. Šejna, and M.Th. van Genuchten. 1999. The HYDRUS-2D software package for simulating the two-dimensional movement of water, heat and multiple solutes in variably-saturated media. *IGWMC-TPS 53. Version 2.0. Int. Ground Water Model. Ctr.*, Colorado School of Mines, Golden.

Skaggs, T.H., T.J. Trout, J. Šimůnek, and P.J. Shouse. 2004. Comparison of HYDRUS-2D simulations of drip irrigation with experimental observations. *J. Irrig. Drain. Eng.* 130:304–310.

Thorburn, P.J., F.J. Cook, and K.L. Bristow. 2003. Soil-dependent wetting from trickle emitters: Implications for system design and management. *Irrig. Sci.* 22:121–127.

Topp, G.C., J.L. Davis, and A.P. Annan. 1980. Electromagnetic determination of soil water content: Measurements in coaxial transmission lines. *Water Resour. Res.* 16:574–582.

Trout, T.J. 2006. Fumigant use in California: Response to the phase-out. *Pap. 18. In Proc. Annu. Int. Res. Conf. on MeBr Alternatives and Emission Reductions*, Orlando, FL, 6–9 Nov. 2006. Available at www.mbao.org/2006/06Proceedings/018TroutTmb-fumuse-06.pdf (verified 7 Aug. 2010). *Methyl Bromide Alternatives Outreach*, Fresno, CA.

Trout, T.J., T.H. Skaggs, and Y. Rothfuss. 2005. Irrigation practices that improve drip fumigation. p. 35-1–35-3. *In Proc. Annu. Int. Res. Conf. on Methyl Bromide Alternatives and Emissions Reductions*, San Diego, 31 Oct.–3 Nov. 2005. Available at mbao.org/2005/05Proceedings/035TroutT%20mb-DripDist-mbao05.pdf (verified 7 Aug. 2010). *Methyl Bromide Alternatives Outreach*, Fresno, CA.

Wang, D., S.R. Yates, F.F. Ernst, and J.A. Knuteson. 2001. Volatilization of 1,3-dichloropropene under different application methods. *Water Air Soil Pollut.* 127:109–123.

Wang, F.-X., Y. Kang, and S.-P. Liu. 2006. Effects of drip irrigation frequency on soil wetting pattern and potato growth in North China Plain. *Agric. Water Manage.* 79:248–264.

Warrick, A.W. 1974. Time-dependent linearized infiltration: I. Point sources. *Soil Sci. Soc. Am. J.* 38:383–386.

Zur, B. 1976. The pulsed irrigation principle for controlled soil wetting. *Soil Sci.* 122:282–291.

Zur, B., and D. Savaldi. 1977. Infiltration under a pulsed water application: I. The nature of the flow system. *Soil Sci.* 124:127–134.